



ELSEVIER

Contents lists available at ScienceDirect

Journal of Luminescence

journal homepage: www.elsevier.com/locate/jlumin

Photoluminescent and structural properties of ZnO containing Eu^{3+} using PEG as precursor



Patrícia M. dos Reis^a, Adriana S. de Oliveira^a, Edison Pecoraro^b, Sidney J.L. Ribeiro^b, Marcio S. Góes^c, Clebio S. Nascimento^d, Rogéria R. Gonçalves^e, Daniela P. dos Santos^a, Marco A. Schiavon^a, Jefferson L. Ferrari^{a,*}

^a Laboratório de Materiais Inorgânicos Fotoluminescentes e Polímeros Biodegradáveis (LAFOP), Grupo de Pesquisa em Química de Materiais (GPQM), Departamento de Ciências Naturais (DCNat), Universidade Federal de São João del-Rei (UFSJ), Campus Dom Bosco, Praça Dom Helvécio, 74, 36301-160 São João del-Rei, MG, Brazil

^b Instituto de Química, UNESP, 14800-060 Araraquara, SP, Brazil

^c Universidade Federal da Integração Latino-Americana (UNILA), Av. Tancredo Neves, 6731 – Bloco 4, P.O. Box. 2044, CEP: 85867-900 Foz do Iguaçu, PR, Brazil

^d Laboratório de Química Teórica e Computacional – (LQTC), Departamento de Ciências Naturais, Universidade Federal de São João del-Rei, Campus Dom Bosco, Praça Dom Helvécio, 74, 36301-160 São João del-Rei, MG, Brazil

^e Departamento de Química, Faculdade de Filosofia, Ciências e Letras de Ribeirão Preto, Universidade de São Paulo, 14040-901 Ribeirão Preto, SP, Brazil

ARTICLE INFO

Article history:

Received 17 March 2015

Received in revised form

25 May 2015

Accepted 16 June 2015

Available online 24 June 2015

Keywords:

Rare earth

Photoluminescence

Zinc oxide

Europium

ABSTRACT

ZnO powders containing different concentrations of Eu^{3+} synthesized using polyethylenoglycol (PEG) as precursor are reported. The viscous solutions were obtained and heated-treated at different temperatures to obtain materials in powder form in order to analyze the influence of temperature on photoluminescent and structural properties. The synthesis proposed in this paper enable the fabrication of the zinc oxide material containing Eu^{3+} with high relative concentrations. TG and DTA analyses allowed the behavior of the decomposition of precursors used in the synthesis to be observed. PEG used as precursor proved to be a very interesting molecule, producing materials with good photoluminescent properties. The structural characteristics of the material were evaluated by X-ray diffraction, followed by a Rietveld refinement. The results obtained show that is possible to incorporate Eu^{3+} in a ZnO host matrix with relatively high concentrations. The cell parameters showed minimal distortion and were independent of Eu^{3+} concentration. From calculation of the band gap, the difference of energy between HOMO and LUMO of 3.28 eV was determined which is in accordance with the literature. The presence of Eu^{3+} makes the material a red emitter and the color of emission is dependent on wavelength of excitation (294 or 463 nm). The excitation at 294 nm promotes the photoluminescence emission in the visible region with large band assigned to the defects present in the ZnO host matrix. However when the material is excited at 463 nm (exactly on Eu^{3+} energy level) bands with intense emission around 612 nm are observed and assigned to the hypersensitive intraconfigurational transition of Eu^{3+} and the large band below that wavelength it is observed. The presence of a large band emission when the samples are excited at 463 nm is an indication of the energy transfer from Eu^{3+} to the ZnO host matrix. The results obtained demonstrate that with this synthesis, the structural and photoluminescent properties of the product make it a potential candidate for applications in solar cells.

© 2015 Elsevier B.V. All rights reserved.

1. Introduction

The optical properties of Rare-Earth ions (RE^{3+}) in arrays of inorganic oxides have received great attention in both the study of fundamental properties and technological development [1–5]. This interest is partly correlated to the versatility of synthesis and

preparation, resulting in a variety of materials with potential applications in many different areas [2,3,5,6].

Among the most studied RE^{3+} , Eu^{3+} shows intense emission of light in the red region of the electromagnetic spectrum [6,7]. The optical properties of this ion is related to the intraconfigurational transitions from f–f energy levels, and the most intense emission is attributed to the hypersensitive transition ${}^3\text{D}_0 \rightarrow {}^7\text{F}_2$ positioned at approximately 612 nm (~ 2.02 eV).

However, to exhibit intense photoluminescent properties, the rare earth ions need to be inserted into adequate host matrix.

* Corresponding author. Tel./fax: +55 32 3379 2481.

E-mail addresses: ferrari@ufsj.edu.br, jeffersonferrari@gmail.com (J.L. Ferrari).

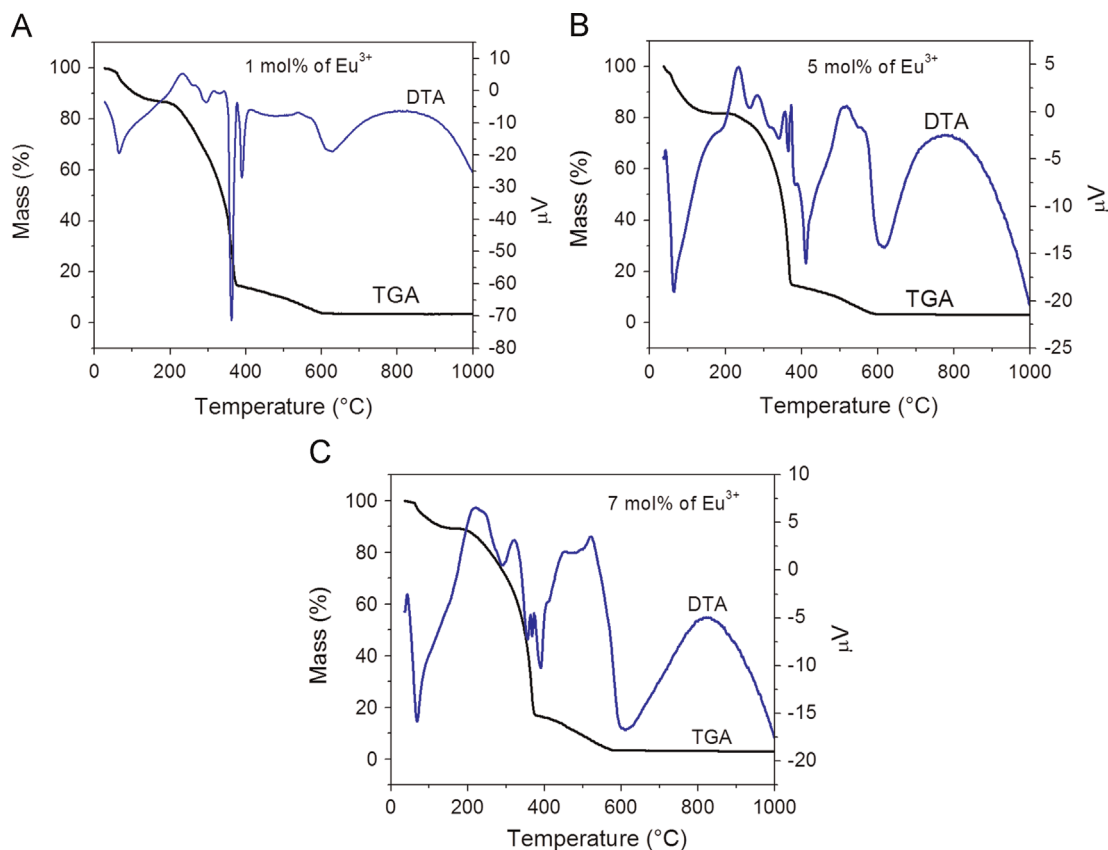


Fig. 1. TGA and DTA analysis of the precursor's solutions containing 1, 5 and 7 mol% of Eu^{3+} with range from room temperature up to 1000 °C.

The intensity of the luminescence exciting directly on RE^{3+} is rather low, because of their low molar absorptivity (Laporte rules). In order to improve their photoluminescent properties, a host matrix that absorbs light can be used to promote energy transfer to the RE^{3+} , resulting in enhancement of luminescence intensity of the rare earth ions. As a consequence, the optical properties are dependent on RE^{3+} emitter and host used as well.

Zinc oxide (ZnO) is a good example of host matrix for trivalent ion activators that feature photoluminescent properties. The primary characteristic of focus in literature for ZnO as a host matrix for different species of ions is the band-gap value presented by this oxide. ZnO has a band gap value around 3.3 eV, which is very interesting for applications in optical devices. The value of the band-gap also is interesting for the introduction of many kind of ions in the structure in attempt to improve already existing properties.

Many studies in the literature have reported on ZnO matrix incorporates low amounts of RE^{3+} due the difference between the ionic radii of Zn^{2+} and RE^{3+} . Pal and Manam (2014) [8] reported about the presence of Li^+ metals in the ZnO host matrix, in which the Li^+ acts as an enhancer of RE^{3+} photoluminescent emission. Koao et al., (2014) [9] studied the effect of the Eu^{3+} concentration on the ZnO nanostructures obtained via a chemical bath deposition (CBD). In these results, the maximum intensity of photoluminescence was observed for samples containing 3 mol% of Eu^{3+} and quenching for higher concentrations this one. Luo et al. (2014) reported the efficient energy transfer from the ZnO host to the RE^{3+} and also between RE^{3+} ($\text{Eu}^{3+}/\text{Tb}^{3+}$) under excitation at 385 nm [10]. Regarding, the effect of the ions on the structure, Yang et al. (2014) reported the decreasing of average particle size as a function of increasing of molar ratio between $\text{Eu}^{3+}/\text{Zn}^{2+}$ from 0.01 to 0.03 [11].

Zinc oxide has a high band-gap values (~ 3.30 eV) and this values depends on the route of synthesis and provides light emission in the green region of the electromagnetic spectrum [12]. Although there may be several types of lattice defects in the crystal structure of ZnO [13,14], the defect Zn_i , due to the presence of interstitial Zn^0 crystal structure, and V^0 due to lack of O^{2-} ions in the crystal structure, are considered predominant. In addition to these characteristics, the ZnO structure is relatively open making easy the incorporation of impurities or dopants into the crystal lattice. Zinc oxide can exhibit emission bands in the regions of ultraviolet, green and yellow [15]. The UV emission is due to the direct recombination of charge carriers, which are responsible for the observed optical properties. In this way, the correlation between the crystalline structure and optical property of the ion emitter that can be incorporated in the crystal structure is of fundamental importance. Zinc oxide has interesting physico-chemical properties, as low dielectric constant, good photoelectric properties and the possibility of obtaining various nanostructures [15]. Therefore, it is of fundamental importance new chemical routes to synthesized and study nano or microstructured crystalline ZnO providing favorable conditions to assist in the incorporation of the larger amount of RE^{3+} ions in the host [8,16–18].

Based on that, this work aims to study the photoluminescent and structural characteristic of the Eu^{3+} incorporated into the matrix of ZnO using PEG as organic polymeric precursor. In our previous work, the use of PEG as a precursor in the synthesis of Er^{3+} -doped Y_2O_3 [19] was verified a high homogeneity of metals in the precursor's solution.

2. Experimental procedure

Initially 0.5 g of $\text{ZnO}_{(s)}$ (Sigma-Aldrich – 99.99%) was added in 40 mL of distilled water and 2.0 ml of concentrated HCl under

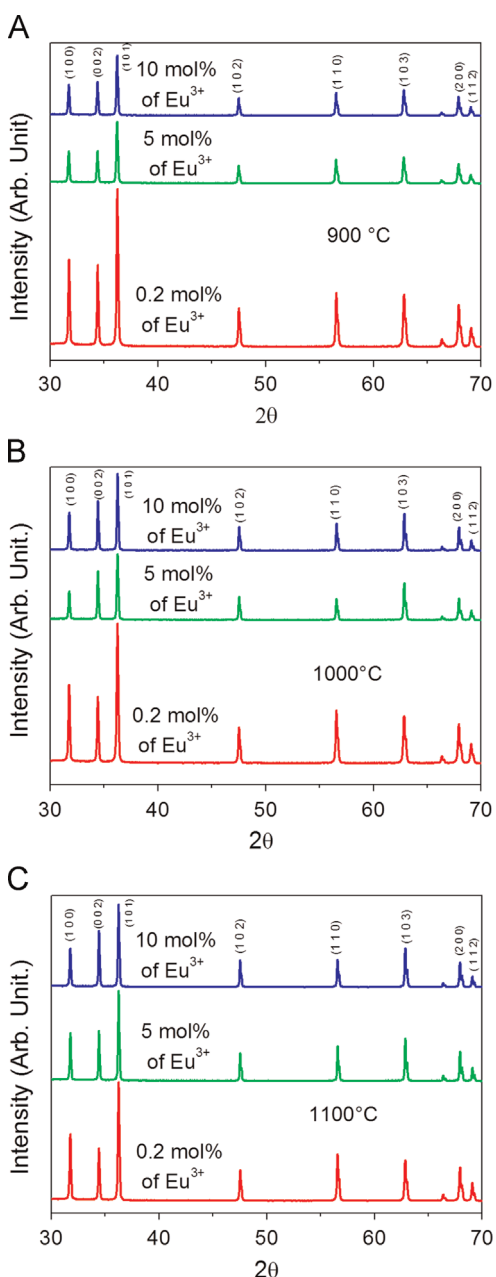


Fig. 2. X ray diffraction of the samples with different amounts of Eu^{3+} heat-treated at: (A) 900, (B) 1000 and (C) 1100 °C.

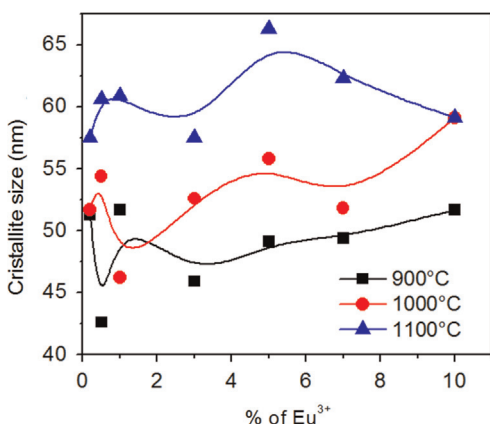


Fig. 3. Crystallite size values of the samples containing different amounts of Eu^{3+} heat-treated at 900, 1000 and 1100 °C.

Table 1
Rietveld agreement indexes.

R indexes	mol% of Eu^{3+}		
	0.5	3	10
R_{wp} (%)	9.67	10.76	11.27
R_{F}^2 (%)	4.96	7.56	8.34
R_{Bragg}	2.46	2.09	2.50
S	1.56	1.58	1.50

Table 2

Phase data and atomic parameters calculated by the Rietveld method for the samples containing 0.5, 3 and 10 mol% of Eu^{3+} and heat-treated at 1100 °C. The special positions x/a and y/b are 1/3 and 2/3, respectively, for all samples.

	0.5 mol%	3 mol%	10 mol%
a (Å)	3.25028(4)	3.25094(4)	3.25091(4)
c (Å)	5.20668(8)	5.20617(9)	5.20600(8)
V (Å ³)	47.636(1)	47.650(2)	47.648(2)
d (g cm ⁻³)	5.674	5.696	6.012
c/a	1.6019	1.6014	1.6014
$\text{Zn}^{2+}/\text{Eu}^{3+}$ (z/c)	0.3933(7)	0.4044(8)	0.41029(0)
O^{2-} (z/c)	0.012137(0)	0.022049(0)	0.02800(6)
Occupancy ($\text{Zn}^{2+}/\text{Eu}^{3+}$)	1	0.996(27)/0.004	0.944(178)/0.056
		(27)	(178)

stirring at 80 °C up to full dissolution. After complete dissolution of $\text{ZnO}_{(s)}$, Eu^{3+} from the chloride solution were added to the solution with 0.2, 0.5, 1, 3, 5, 7 and 10 mol% relative to the total number of moles of Zn^{2+} . Polyethylene glycol (PEG – Synth – 99.9%) was added at molar concentration 5 times higher than the sum of the molar concentration of Zn^{2+} and Eu^{3+} . The solutions were kept under stirring at 80 °C so that partial evaporation of the solvent left viscous solutions. The viscous solutions were submitted to the thermogravimetric analyzes and differential thermal analysis (TGA/DTA). A thermo analyzer Shimadzu model DTG-60H with a heating rate of 10 °C/min under air atmosphere from room temperature up to 1000 °C was used. Based on the behavior of the thermograms, the viscous solutions were heat-treated at 900, 1000 and 1100 °C for 4 h. The x-ray diffraction (XRD) analyses were used to obtain information about the crystalline structure of the material after heat-treatment. The measurements were performed on a SHIMATZU diffractometer XDR-600 operated at 30 kV and 30 mA. Cu-radiation ($\text{Cu K}\alpha$, $\lambda=1.5418$ Å) with graphite monochromator has been used. The data was collected in Bragg–Brentano mode within the range $15^\circ \leq 2\theta \leq 80^\circ$. The data was collected with 0.02° (2θ) steps with a fixed-time of 2 s. The refinement of XRD diffraction results was performed using the Rietveld's profile analysis method [20], with the General Structure Analysis System (GSAS) program suite [21], with XPGUI interface [22]. The following parameters were refined: atomic coordinates, occupancies, unit cell, scale factor, sample displacement, atomic displacement and Full Width at Half Maximum (FWHM). The peak profile function was modeled using a convolution of the Thompson–Cox–Hastings pseudo-Voigt function (pV-TCH) [23], using the asymmetry function described by Finger et al. (1994) [24]. The crystal structure parameter was used as basis of the database code ICSD: 94002 (ZnO). Based on the diffractograms, the crystallite size was calculated using Scherrer's equation. The photoluminescent spectra were collected at room temperature using a spectrofluorimeter Fluorolog SPEX F2121/Jobin-Yvon, 450 W ozone free Xenon lamp as a source, and the Hamamatsu R928 photomultiplier as a detector. The excitation and emission slits were fixed at 0.3 and 0.5 nm, respectively. The wavelengths of excitation were fixed at 394 or 463 nm.

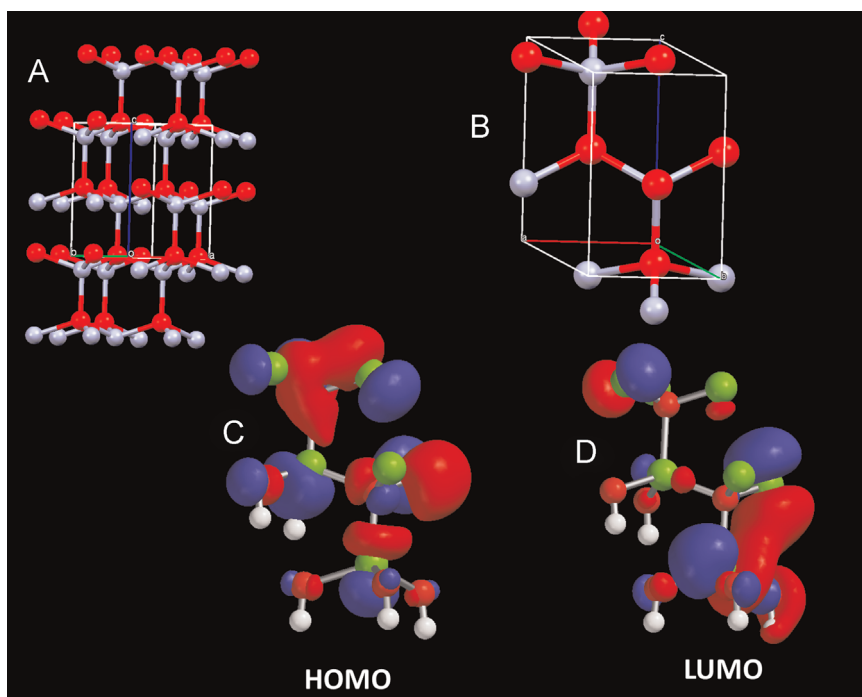


Fig. 4. (A) Structure of ZnO, (B) unit cell of ZnO, (C) HOMO and (D) LUMO orbitals.

3. Results and discussions

To obtain information about the thermal stability of the viscous solutions used as precursor, and also about the temperature to obtain the final product, the samples containing 1, 5 and 7 mol% of Eu^{3+} were submitted to TGA and DTA analyzes, and the results are shown in Fig. 1.

The results show that the steps present in the thermogravimetric analyzes can be assigned to the decomposition of the organic matter from PEG used as precursor in the synthesis of the viscous solutions. The first loss of mass refers to the elimination of water, occurring between 100 and 200 °C. The second event between 250 and 380 °C is assigned to the loss of organic matter connected weakly with the metals ions, and the third one, between 600 and 1000 °C is assigned to the degradation of organic matter linked most strongly with metals ions. The yield of the synthesis was around 2.7% of the final material after thermal treatment at 1000 °C. In this work, relatively large amounts of PEG as a precursor was used to prepare the viscous solutions in relation to the amount of RE^{3+} , in order to promote the homogeneity or high dispersion among metals presents in the precursor solution. In the DTA analyzes, all behavior is verified to be due to the endothermic events during the decomposition of the precursors. As observed in DTA curve, the viscous solution containing 1 and 3 mol% of Eu^{3+} presents a narrow peak between 380 and 400 °C that can be associated to the some type of solvent-structuration or even the formation of some kind of complex. For viscous solution containing 5 mol% of Eu^{3+} , this peak is broader.

Based on the behavior observed in the TG and DTA analyzes all viscous solutions containing 0.2, 0.5, 1, 3, 5, 7 and 10 mol% of Eu^{3+} were thermally heated-treated at 900, 1000, and 1100 °C for 4 h. The diffractograms of the heat-treated samples, Fig. 2, shows the formation of the crystalline phase of the ZnO wurtzite type, belonging to the space group $P6_3mc$ in accordance to database code ICSD: 94002. No peaks related to secondary phases were detected. These results suggest that little fraction of Eu^{3+} are inserted into lattice or located as clusters on the surface of ZnO particles. In the wurtzite structure Zn^{2+} lying in a tetrahedral

symmetry, surrounded by four oxygen atoms. It is known that the ionic radius of the Eu^{3+} localized in symmetry equal 6 is 1.087 Å and for symmetry equal 4, as in wurtzite phase, is 0.740 Å. Taking into account that the wurtzite presents an open structure with interstices that can accommodate the Eu^{3+} , it is valid to suppose that RE^{3+} are not replacing or displacing Zn^{2+} in the crystalline structure. Although differences of ionic radii between Zn^{2+} and Eu^{3+} in different sites of symmetries do not cause changes in the crystalline wurtzite structure, the small influence on structure parameters by rare earth addition is discussed below.

Based on the reflection peak positioned at $2\theta=36.26^\circ$, attributed to the (101) Miller plane, and using the Scherrer's equation (Eq. (1)), the average of nanocrystallite size may be calculated. In Scherrer's equation, D is the average diameter of the crystallites, B is dependent on the particle shape factor (usually 0.89 for spherical shapes), β is the full width half maximum of the peak of diffraction and θ is the diffraction angle. Fig. 3 shows that the nanocrystallite size increases as a function of the temperature of heat-treatment. The increase of crystallite size can in a way contribute to decrease defects in the crystal structure.

The additional energy related to the increment on the temperature of the heat treatments contributes to the coalescence between the nanocrystallites, resulting in nanocrystallites with larger sizes. A tendency of increasing the nanocrystallite size as a function of increasing amount of Eu^{3+} in the system is also verified.

$$D = \frac{B\lambda}{\beta \cos \theta} \quad (1)$$

Table 1 shows the Rietveld refinement indexes, and the lattice parameters. Volume, atomic positions, and density are shown in Table 2 obtained by Rietveld refinement for ZnO containing Eu^{3+} samples heat-treated at 1100 °C. The analysis of phases through the Rietveld method indicates 100 wt% of ZnO phase (space group= $P6_3mc$) and the likely incorporation of large amount of Eu^{3+} into the lattice of ZnO (probably in the interstices of the wurtzite structure). The results, Table 2, show that the presence of Eu^{3+} induces small variations in the cell parameters as a function

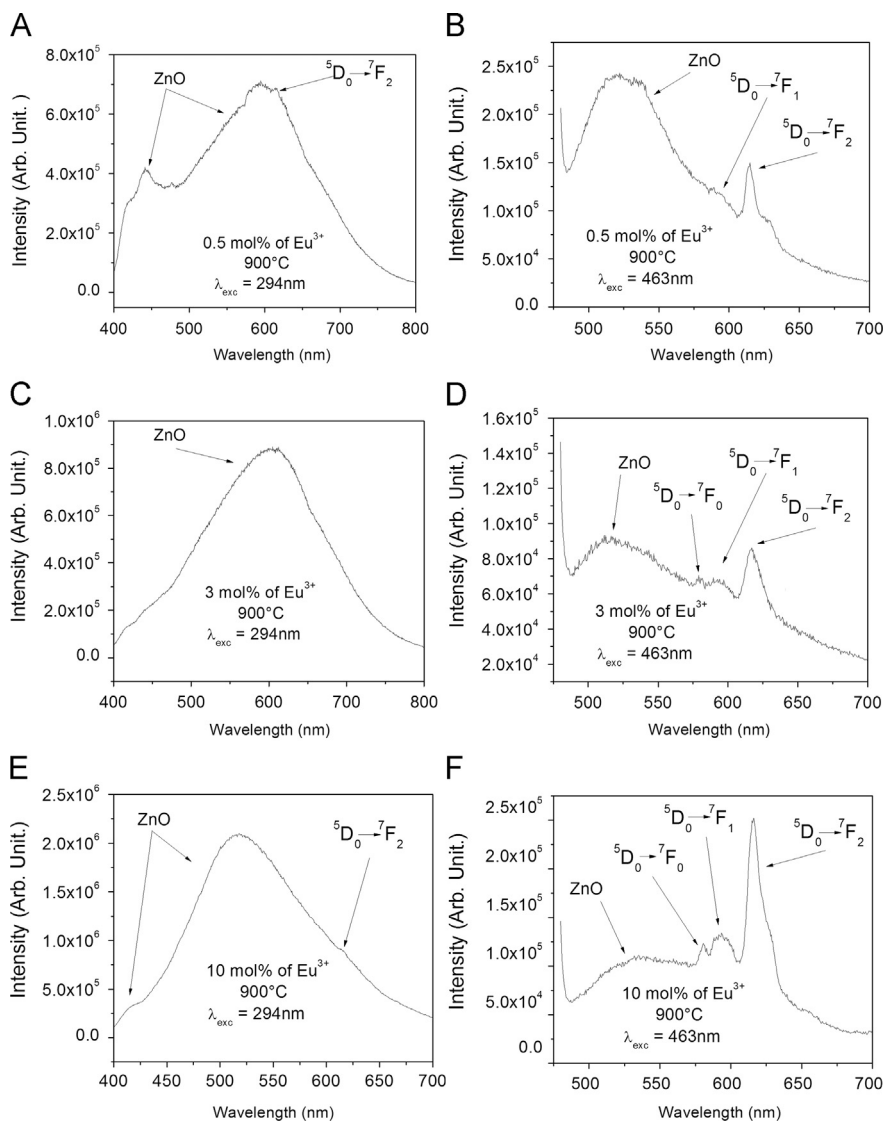


Fig. 5. Emission spectra under excitation at (A), (C) and (E) 294 nm, and (B), (D) and (F) at 463 nm of the samples containing different amount of Eu^{3+} heat-treated at 900 °C.

of incorporation Eu^{3+} in the ZnO structure. On the other hand, the increasing of Eu^{3+} concentration causes the decrease of the values c/a (tetragonal distortions) and increase z/c atomic position. The results suggest tetragonal distortions (from $c/a=1.6019$ to $c/a=1.6014$) is slightly smaller for the samples with higher Eu^{3+} concentration and can be correlated to the incorporation of low quantity of Eu^{3+} in position of atomic Zn^{2+} . The z/c atomic position leads to an increase in Zn/Eu–O distances, from 1.9851(36) Å to 1.9902(113) Å.

Based on the results obtained by the Rietveld refinement we were able to calculate the theoretical band-gap energy for Eu^{3+} -doped ZnO using the unit cell depicted in Fig. 4(A and B). The band-gap energy was estimated at semi empirical Sparkle/PM7 level of theory by solid-state calculation [25]. The theoretical band-gap obtained in this work from the difference of energy between HOMO and LUMO, Fig. 4(C and D), respectively, is 3.28 eV, which is in good agreement with other work reported in literature [15]. These results emphasize the capability of the use of the Sparkle model for the prediction of physical chemical properties containing within the PM7 semi empirical model.

The incorporation of RE^{3+} in solid matrices provide the photoluminescent emission assigned to the internal 4f transitions, and are observed for samples heat-treated at 1100 °C and excited at

463 nm in Fig. 5(B, D and F) and Fig. 6(B, D and F). It is also observed that samples heat-treated at 900 and 1100 °C and excited at 294 nm show large emission band with maximum of intensity positioned around 530 nm (~ 2.34 eV), as show in Fig. 5(A, C and E) and Fig. 6(A, C and E). The excitation at 293 nm was chosen specifically to direct excitation of the ZnO matrix. This emission band can be assigned to the O^{2-} vacancy, and other band with a maximum around 425 nm can be assigned to the Zn^{2+} vacancy. In contrast to Jia et al., (2003) [26] the compound based on $\text{ZnO}:1\%\text{EuF}_3, \text{Li}^+$, when excited in the UV region, shows energy transfer from the host to the Eu^{3+} . In this work, when the materials are excited at 463 nm, exactly in the Eu^{3+} energy levels, a large band emission is observed around 530 nm, which can be assigned to the oxygen vacancy and the bands localized at 578 nm (${}^5\text{D}_0 \rightarrow {}^7\text{F}_0$), 590 nm (${}^5\text{D}_0 \rightarrow {}^7\text{F}_1$), 613 nm (${}^5\text{D}_0 \rightarrow {}^7\text{F}_2$), are assigned to the Eu^{3+} . This behavior is an indication of energy transfer from Eu^{3+} to the ZnO host matrix, due to the intense emission band centered at 530 nm assigned to the ZnO. The presence of small inhomogeneous broadening of the band assigned to the ${}^5\text{D}_0 \rightarrow {}^7\text{F}_0$ of Eu^{3+} can be associated to the Eu^{3+} locate in one site of symmetry with small distortions. Commercial Si solar cells and/or dyes generally absorb energy in the ultraviolet and visible region of electromagnetic spectrum. However, part of this energy absorbed

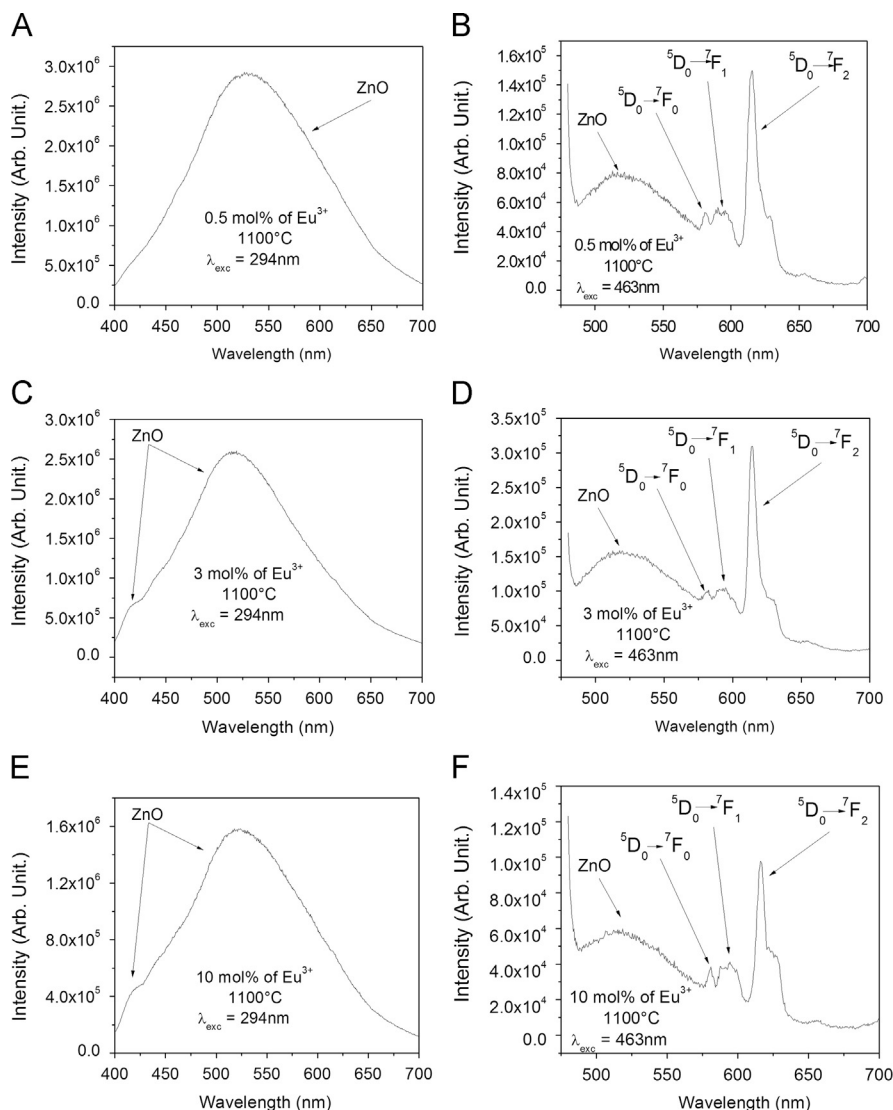


Fig. 6. Emission spectra under excitation at (A), (C) and (E) 294 nm, and (B), (D) and (F) at 463 nm of the samples containing different amount of Eu^{3+} heat-treated at 1100°C .

can be dissipated in the system via non-radiative processes, as thermalization for instance. One way to contribute to increase the efficiency conversion in solar cells is to improve the electron injection in the conduction band of the present semiconductor in solar cells. In this sense, systems that absorb energy in the ultraviolet and/or visible region promoting emission in the region where the solar cells absorb can be a solution for improving the energy conversion. For the system presented in this work, it must be taken into account that if properly applied in solar cells, can absorb energy in the ultraviolet, 294 nm and in the region of 463 nm simultaneously and promote maximum of emission in the visible region of 525 and 612 nm. This region has efficient absorption by the commercial solar cells, which can result in improvement of efficiency in converting light into electric current.

The emission intensity may be affected by the amount of dopant within the system. The greater distance between the dopant ions can contribute to the smaller effect of cross relaxation process. The increasing of distance among ions may be caused by an increasing in amounts of structural defects. Therefore the samples containing higher amounts of Eu^{3+} heat-treated at 900°C exhibit greater relative emission intensity in comparison to the emission of the matrix. This effect can be related to the fact that defects contribute to the increasing of distance of ions decreasing the effect of cross relaxation

and energy migration. Otherwise the samples heat-treated at 1100°C have higher relative emission intensities for samples with less Eu^{3+} and no concentration quenching effect was observed increasing the Eu^{3+} concentration, strongly indicating the high dispersion of rare earth ions in the ZnO structure, avoid non-radiative relaxation due to energy migration and cross relaxation.

4. Conclusion

The method of synthesis used in this work was effective and easy for obtaining ZnO wurtzite-phase containing RE^{3+} with photoluminescent properties. The Rietveld refinement shows that the incorporation of Eu^{3+} does not cause significantly changes in the structure parameters, only enough to indicate that rare earth ions are incorporated into the host structure, with any evidence of rare earth cluster formation. The samples emission depends on excitation wavelength, *i.e.*, when excited at 294 nm, the photoluminescence of the ZnO host matrix is predominant. On the other hand, the emission exhibited after excitation of the Eu^{3+} (at 463 nm), suggests a process of energy transfer to the ZnO host, yielding the addition of an electron in the conduction band of the ZnO. Finally, the properties observed for ZnO: Eu^{3+} compounds

make them potential candidate for UV-Visible energy converters, i.e., absorbers of energy in the UV region generating emission in the visible region.

Acknowledgments

The authors would like to acknowledge FAPEMIG, FAPESP, CAPES, and CNPq. This work is a collaboration research project of members of the Rede Mineira de Química (RQ-MG) supported by FAPEMIG (Project: REDE-113/10).

References

- [1] G. Blasse, B.C. Grabmaier, *Luminescent Materials*, Springer-Verlag, Berlin, 1994.
- [2] J.L. Ferrari, K.D. Lima, E. Pecoraro, R.A.S. Ferreira, L.D. Carlos, R.R. Goncalves, *J. Mater. Chem.* 22 (2012) 9901.
- [3] Y. Ledemi, M. El Amraoui, J.L. Ferrari, P.L. Fortin, S.J.L. Ribeiro, Y. Messaddeq, *J. Am. Ceram. Soc.* 96 (2013) 825.
- [4] C.S. Cunha, J.L. Ferrari, D.C. de Oliveira, L.J. Queiroz Maia, A.S. Leonidas Gomes, S.J. Lima Ribeiro, R.R. Goncalves, *Mater. Chem. Phys.* 136 (2012) 120.
- [5] J.L. Ferrari, R.L.T. Parreira, A.M. Pires, S.A.M. Lima, M.R. Davolos, *Mater. Chem. Phys.* 127 (2011) 40.
- [6] J.L. Ferrari, M.A. Cebim, A.M. Pires, M.A.C. dos Santos, M.R. Davolos, *J. Solid State Chem.* 183 (2010) 2110.
- [7] J.L. Ferrari, M.A. Schiavon, R.R. Goncalves, A.M. Pires, M.R. Davolos, *Thin Solid Films* 524 (2012) 299.
- [8] P.P. Pal, J. Manam, *J. Lumin.* 145 (2014) 340.
- [9] L.F. Koao, F.B. Dejene, R.E. Kroon, H.C. Swart, *J. Lumin.* 147 (2014) 85.
- [10] L. Luo, F.Y. Huang, G.S. Dong, H.H. Fan, K.F. Li, K.W. Cheah, J. Chen, *Opt. Mater.* 37 (2014) 470.
- [11] L. Yang, Z. Jiang, J. Dong, A. Pan, X. Zhuang, *Mater. Lett.* 129 (2014) 65.
- [12] P.M. Shirage, *Mater. Today* 16 (2013) 505.
- [13] S.A.M. Lima, F.A. Sigoli, M. Jafelicci, M.R. Davolos, *Int. J. Inorg. Mater.* 3 (2001) 749.
- [14] F.A. Sigoli, C.O. Paiva-Santos, M. Jafelicci, M.R. Davolos, *Powder Diffr.* 16 (2001) 153.
- [15] L. Schmidt-Mende, J.L. MacManus-Driscoll, *Mater. Today* 10 (2007) 40.
- [16] W.M. Jadwisieniczak, H.J. Lozykowski, A. Xu, B. Patel, *J. Electron. Mater.* 31 (2002) 776.
- [17] P.P. Pal, J. Manam, *Radiat. Phys. Chem.* 88 (2013) 7.
- [18] S.A.M. Lima, F.A. Sigoli, M.R. Davolos, *J. Solid State Chem.* 171 (2003) 287.
- [19] R.V. Perrella, D.P. dos Santos, G.Y. Poirier, M.S. Góes, S.J.L. Ribeiro, M.A. Schiavon, J.L. Ferrari, *J. Lumin.* 149 (2014) 7.
- [20] H.M. Rietveld, *J. Appl. Crystallogr.* 2 (1969) 65.
- [21] A.C. Larson, R.B. Von Dreele, *General Structure Analysis System (GSAS)*, Los Alamos National Laboratory Report LAUR 86-748, 2004.
- [22] B.H. Toby, *J. Appl. Crystallogr.* 34 (2001) 210.
- [23] R.A. Young, P. Desai, *Arch. Nauk. Mater.* 10 (1989) 19.
- [24] L.W. Finger, D.E. Cox, A.P. Jephcoat, *J. Appl. Crystallogr.* 27 (1994) 892.
- [25] J.D.L. Dutra, M.A.M. Filho, G.B. Rocha, R.O. Freire, A.M. Simas, J.J.P. Stewart, *J. Chem. Theory Comput.* 9 (2013) 3333.
- [26] W. Jia, K. Monge, F. Fernandez, *Opt. Mater.* 23 (2003) 27.